



## Dipolar filtered $^1\text{H}$ - $^{13}\text{C}$ heteronuclear correlation spectroscopy for resonance assignment of proteins

X.L. Yao & M. Hong\*

*Department of Chemistry, Iowa State University, Ames, IA 50011, U.S.A.*

Received 7 February 2001; Accepted 9 May 2001

*Key words:* HETCOR,  $^1\text{H}$  chemical shift, resonance assignment, selective labeling, uniform labeling

### Abstract

Resonance assignment is necessary for the comprehensive structure determination of insoluble proteins by solid-state NMR spectroscopy. While various 2D and 3D correlation techniques involving  $^{13}\text{C}$  and  $^{15}\text{N}$  spins have been developed for this purpose,  $^1\text{H}$  chemical shift has not been exploited sufficiently. We demonstrate the combination of the regular  $^1\text{H}$ - $^{13}\text{C}$  heteronuclear correlation (HETCOR) experiment and a dipolar filtered HETCOR technique to obtain better resolved  $^1\text{H}$  chemical shift spectra. The dipolar filtered experiment, MELODI-HETCOR, simplifies the  $^1\text{H}$  spectra by suppressing the directly bonded C-H correlation peaks and retaining only the medium- and long-range cross peaks. We apply this MELODI-HETCOR technique to several amino acids and proteins with various isotopic labeling patterns. The enhanced  $^1\text{H}$  chemical shift resolution allows the assignment of overlapping  $\text{H}\alpha$  and  $\text{H}\beta$  resonances in Ser, identifies the  $^1\text{H}$  chemical shift differences between neutral and cationic imidazole rings of His, and permits the assignment of residues with side chain nitrogen atoms in ubiquitin. The potential utility of this dipolar filtered HETCOR technique to resonance assignment of extensively labeled proteins is discussed.

### Introduction

Resonance assignment of proteins in the solid state is becoming an increasingly important topic in solid-state NMR, as the need for comprehensive structure determination has motivated the extensive  $^{13}\text{C}$  and  $^{15}\text{N}$  labeling of proteins to complement traditional site-specific labeling. Many multidimensional correlation techniques involving  $^{13}\text{C}$  and  $^{15}\text{N}$  nuclei have been explored and demonstrated on small peptides and proteins (Hong, 1999; Hong and Griffin, 1998; Ishii and Tycko, 2000; Marassi and Opella, 2000; McDermott et al., 2000; Pauli et al., 2000; Rienstra et al., 2000; Straus et al., 1998; Tan et al., 1999; Wang et al., 2000). However, the  $^1\text{H}$  chemical shifts have not been fully utilized, even though  $^1\text{H}$  and  $^{13}\text{C}$  correlation spectroscopy of small model compounds, conducted with  $^1\text{H}$  homonuclear decoupling for the indirect dimension, has been demonstrated before (Caravatti et al.,

1983; Lee and Griffin, 1989; Lesage et al., 1998; van Rossum et al., 1997). This limitation persists despite the fact that the sensitivity of  $^1\text{H}$ -X heteronuclear correlation is much higher than the correlation of two low-frequency nuclear spins. The main reason for the limited use of  $^1\text{H}$  chemical shifts for protein resonance assignment is the low  $^1\text{H}$  spectral resolution: the  $^1\text{H}$  chemical shift dispersion is about 12 ppm, while the typical  $^1\text{H}$  linewidth achievable under homonuclear decoupling and magic-angle spinning is at best 0.5 ppm for a non-crystalline solid. The ratio between the two is much less favorable compared to  $^{13}\text{C}$  and  $^{15}\text{N}$  spectra of proteins. Apart from the linewidths, another factor contributing to the low  $^1\text{H}$  resolution is that the traditional  $^1\text{H}$ - $^{13}\text{C}$  correlation spectra contain redundant information: a peak correlating a directly bonded proton (e.g.,  $\text{H}\alpha$ ) and carbon (e.g.,  $\text{C}\alpha$ ) does not yield more assignment than the carbon chemical shift alone, which is already characteristic of the amino acid type. For distinguishing different amino acids, the side chain  $^1\text{H}$  chemical shifts are more informative than the backbone  $\text{H}\alpha$  and  $\text{H}^{\text{N}}$ . These side

\*To whom correspondence should be addressed. E-mail: mhong@iastate.edu

chain protons can have correlation peaks with  $C\alpha$  in a dipolar HETCOR spectrum. However, these indirect correlations are often masked by the strong one-bond correlation peaks such as  $C\alpha-H\alpha$ . Therefore, the removal of one-bond correlation peaks will be useful for resolving medium- and long-range correlations to extract more resonance assignment.

To obtain the medium- and long-range C-H correlation peaks in better resolved HETCOR spectra, we have recently introduced a MELODI-HETCOR (medium- and long-distance heteronuclear correlation) technique (Yao et al., 2001). This technique suppresses the one-bond  $^1H-^{13}C$  correlation peaks by dephasing the  $^1H$  magnetization under the strong dipolar coupling to the nearby  $^{13}C$  spin. Those protons without a directly bonded  $^{13}C$  will not dephase, thus their correlations with the far-away  $^{13}C$  spins are preserved. In this way, the  $^1H-^{13}C$  correlation spectra are considerably simplified, and previously low-intensity long-range correlation peaks can be emphasized.

In the current work, we compare the traditional HETCOR spectra and the MELODI-HETCOR spectra of several model systems in detail. These include unlabeled amino acids with small  $^1H$  chemical shift dispersions or complex chemical shift patterns, selectively and extensively labeled proteins, and a uniformly  $^{13}C$  and  $^{15}N$  labeled amino acid. All these experiments involved  $^1H$  homonuclear decoupling. We show that the MELODI filter achieves the amino acid type assignment efficiently. In particular, residues with side chain nitrogen atoms are accentuated by the MELODI dipolar filter.

## Materials and methods

### Materials

The natural abundance amino acids serine, histidine, and histidine hydrochloride monohydrate were obtained from Sigma and used without further purification. 72 mg of Ser and 81 mg of His were packed into two 4-mm magic-angle spinning (MAS) rotors. The experiments on histidine hydrochloride monohydrate were carried out with a 7-mm MAS probe, and about 320 mg of material was used.

Selectively and extensively (S&E)  $^{13}C$  labeled ubiquitin, expressed with  $[2-^{13}C]$  glycerol as the carbon precursor (Hong, 1999), was obtained from VLI Research (Malvern, PA). This S&E  $^{13}C$  labeling pattern reduces the line broadening caused by the

one-bond C-C J-couplings and simplifies the spectral assignment. The synthesis and purification were described previously (Hong, 1999).  $[2-^{13}C]$  glycerol labels all backbone  $C\alpha$  sites except for Leu, thus 67 out of 76 residues in ubiquitin are  $^{13}C\alpha$  labeled. For amino acids produced from the glycolysis pathways (G, C, S, A, L, V, H, F, Y, W), most side chain carbons are unlabeled. The exceptions are Leu ( $\beta$ ,  $\gamma$ ), Val ( $\alpha$ ,  $\beta$ ), and the three aromatic amino acids. In comparison, for amino acids produced from the citric-acid cycle (E, Q, P, R, D, N, M, T, K, I), both the backbone and the side chains are extensively labeled at reduced levels of 50% or lower. About 25 mg of 30% (w/w) hydrated ubiquitin was used.

Colicin Ia channel domain, a 22 kDa protein, was expressed and  $^{13}C$ -labeled using the TEASE protocol (Hong and Jakes, 1999). This labeling scheme further simplifies the NMR spectra by blocking the labeling of the 10 citric-acid cycle amino acids through feedback inhibition. With  $[2-^{13}C]$  glycerol as the carbon precursor, the labeled carbon sites are: H ( $\delta 2$ ), S ( $\alpha$ ), G ( $\alpha$ ), C ( $\alpha$ ), W ( $\alpha$ ,  $\delta 2$ ,  $\zeta 3$ ), F ( $\alpha$ ,  $\gamma$ ,  $\epsilon 1$ ), Y ( $\alpha$ ,  $\gamma$ ,  $\epsilon 1$ ), A ( $\alpha$ ), V ( $\alpha$ ,  $\beta$ ), and L ( $\beta$ ,  $\gamma$ , CO). The number of partially  $^{13}C$  labeled residues is 110, out of a total 189 residues. Thus, TEASE  $^{13}C$  labeling reduces the effective size of the protein by almost half and facilitates the amino acid-type assignment. About 5 mg of 30% (w/w) hydrated protein was used. The protein is in the water-soluble form free of lipids.

### NMR experiments

All NMR experiments were carried out on a Bruker DSX-400 spectrometer (Karlsruhe, Germany) operating at a resonance frequency of 400.49 MHz for  $^1H$ , 100.72 MHz for  $^{13}C$ , and 40.58 MHz for  $^{15}N$ . Two MAS probes with a 4-mm and a 7-mm spinning module were used.

The conventional  $^1H-^{13}C$  HETCOR experiment was carried out based on the sequence of Ernst and co-workers (Caravatti et al., 1983). The  $^1H-^{13}C$  homonuclear interaction was decoupled using the frequency-switched Lee-Goldburg (FSLG) sequence (Lee and Goldburg, 1965). The FSLG decoupling was carried out with a linear phase ramp (Vinogradov et al., 1999), which consists of repetitive phase sweeps from  $0^\circ$  to  $210^\circ$  and from  $30^\circ$  to  $-180^\circ$ . The duration of each ramp unit was synchronized with two  $360^\circ$  pulses around the FSLG effective field, which is tilted at the magic angle with respect to the magnetic field direction. The strength of the effective field was

90.9 kHz for the 4-mm probe and 60.6 kHz for the 7-mm probe, which corresponded to an 11  $\mu$ s and 16.5  $\mu$ s  $360^\circ$ -pulse, respectively. Lee-Goldburg spin lock was applied on the  $^1\text{H}$  channel during cross polarization (CP) (van Rossum et al., 2000) to suppress  $^1\text{H}$  spin diffusion. Typical  $^1\text{H}$  spin-lock field strengths were 45 kHz (41 kHz) on the 4-mm (7-mm) MAS probe. The  $^1\text{H}$  TPPM decoupling field strength during acquisition was about 72 kHz and 52 kHz for the 4-mm and 7-mm MAS probes, respectively. Typical  $^1\text{H}$  and  $^{13}\text{C}$   $90^\circ$  pulse lengths were 3.37  $\mu$ s and 3.9  $\mu$ s, respectively.

The Ser  $^1\text{H}$  chemical shifts were externally referenced to TMS through the Ala H $\beta$  peak (1.32 ppm). A HETCOR experiment on an equimolar mixture of Ala and Ser was done as an intermediate step of referencing. The Ala H $\beta$  chemical shifts were also used to reference the colicin spectra. The ubiquitin  $^1\text{H}$  chemical shifts were referenced to the solution NMR values through the well defined Ile H $\delta$  peaks (Wang and Bax, 1996). The His and Gln  $^1\text{H}$  chemical shifts were referenced to the typical solution NMR values (Wüthrich, 1986). In all the HETCOR and MELODI-HETCOR spectra shown here, peak assignment is indicated by one-letter amino acid symbols, followed by two Greek letters referring to the carbon and proton positions, sequentially. Unknown amino acid identities are represented by an X.

#### *MELODI-HETCOR pulse sequence*

The pulse sequence of the MELODI-HETCOR experiment (Figure 1) consists of a constant  $^1\text{H}$ - $^{13}\text{C}$  dipolar filter period,  $^1\text{H}$  chemical shift evolution ( $t_1$ ), Lee-Goldburg CP, and  $^{13}\text{C}$  detection ( $t_2$ ) (Yao et al., 2001). During the dipolar filter period, the  $^{13}\text{C}$ - $^1\text{H}$  dipolar interaction was recoupled by a  $^{13}\text{C}$   $180^\circ$  pulse during each rotation period, while the  $^1\text{H}$ - $^1\text{H}$  homonuclear interaction and  $^1\text{H}$  chemical shift were averaged by FSLG decoupling and a  $^1\text{H}$   $180^\circ$  pulse, respectively. The extent of heteronuclear dipolar dephasing was regulated by the position of the  $^{13}\text{C}$   $180^\circ$  pulse in the rotation period ( $t_f$ ). The  $^1\text{H}$  chemical shift evolution occurred under FSLG decoupling. At the end of the evolution period, a  $^1\text{H}$   $35^\circ$   $-y$  pulse rotated the cosine-modulated magnetization to the  $z$ -axis. A subsequent  $90^\circ$  pulse with alternating phases then rotated it back to the transverse plane. The last  $35^\circ$   $+y$  pulse rotated the  $z$ -magnetization to the effective field of the LG spin-lock pulse to prepare for polarization transfer to  $^{13}\text{C}$ . The indirect  $^1\text{H}$  dimension was recorded in an

off-resonance manner using only the cosine dataset. In comparison, the HETCOR spectra were acquired using the States-TPPI detection scheme for the indirect dimension.

## **Results and discussion**

### *Serine*

We chose Ser to demonstrate the spectral simplification and resolution enhancement of MELODI-HETCOR over the traditional HETCOR experiment, because Ser H $\alpha$  and H $\beta$  have relatively similar chemical shifts. Figure 2 shows the Ser HETCOR spectra with and without the C-H dipolar filter. In the conventional HETCOR spectra (Figure 2a), both the C $\alpha$  and C $\beta$  cross sections show a broad  $^1\text{H}$  signal around 4 ppm, indicating that the H $\alpha$  and H $\beta$  peaks overlap. The application of the  $^{13}\text{C}$ - $^1\text{H}$  MELODI filter yielded a spectrum with clearly different aliphatic  $^1\text{H}$  frequencies between the two cross sections (Figure 2b). The resolved H $\alpha$  and H $\beta$  chemical shifts differ by only about 0.6 ppm (Figures 2c and d). Further, the H $\alpha$  peak is upfield from the H $\beta$  peak, in contrast to most other amino acids. This illustrates the importance of resolving the  $^1\text{H}$  signals by filtering out the directly bonded correlation peaks. The MELODI-HETCOR spectrum of Ser was acquired with a LG-CP contact time of 1 ms, during which  $^1\text{H}$  spin diffusion was inactive. However, even if normal Hartmann-Hahn CP were used such that  $^1\text{H}$  spin diffusion was active, the directly-bonded correlation peaks such as C $\alpha$ -H $\alpha$  and C $\beta$ -H $\beta$  would still be suppressed, since the  $^1\text{H}$  frequencies have already been encoded by the time CP begins.

Both the HETCOR and MELODI-HETCOR spectra of Ser show correlation peaks at downfield proton frequencies of about 8 ppm. For the C $\alpha$  slice, the intensity must originate from the amino protons, which are not dephased by the  $^{13}\text{C}$ - $^1\text{H}$  dipolar filter. For the C $\beta$  slice, on the other hand, the 8-ppm peak may include both H $^{\text{N}}$  and OH contributions.

### *Histidine*

His is representative of amino acids with ring carbons in the side chain. Figures 3a and b show its  $^1\text{H}$ - $^{13}\text{C}$  HETCOR and MELODI-HETCOR spectra, where peaks originating from both directly bonded and indirectly bonded spin pairs are observed. In the aliphatic carbon region, H $\alpha$  and H $\beta$  cross peaks are

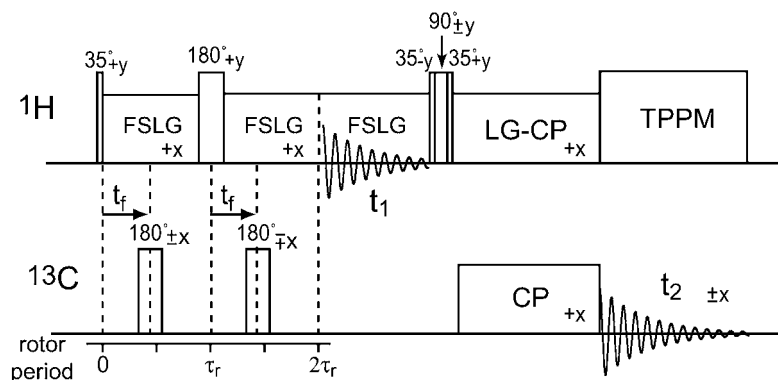


Figure 1. Pulse sequence for the MELODI-HETCOR experiment. The  $^1\text{H}$  magnetization is dephased by the  $^{13}\text{C}$ - $^1\text{H}$  dipolar coupling for two rotor periods before evolving under the chemical shift interaction.  $^{13}\text{C}$  detection follows a Lee-Goldburg CP from  $^1\text{H}$ .

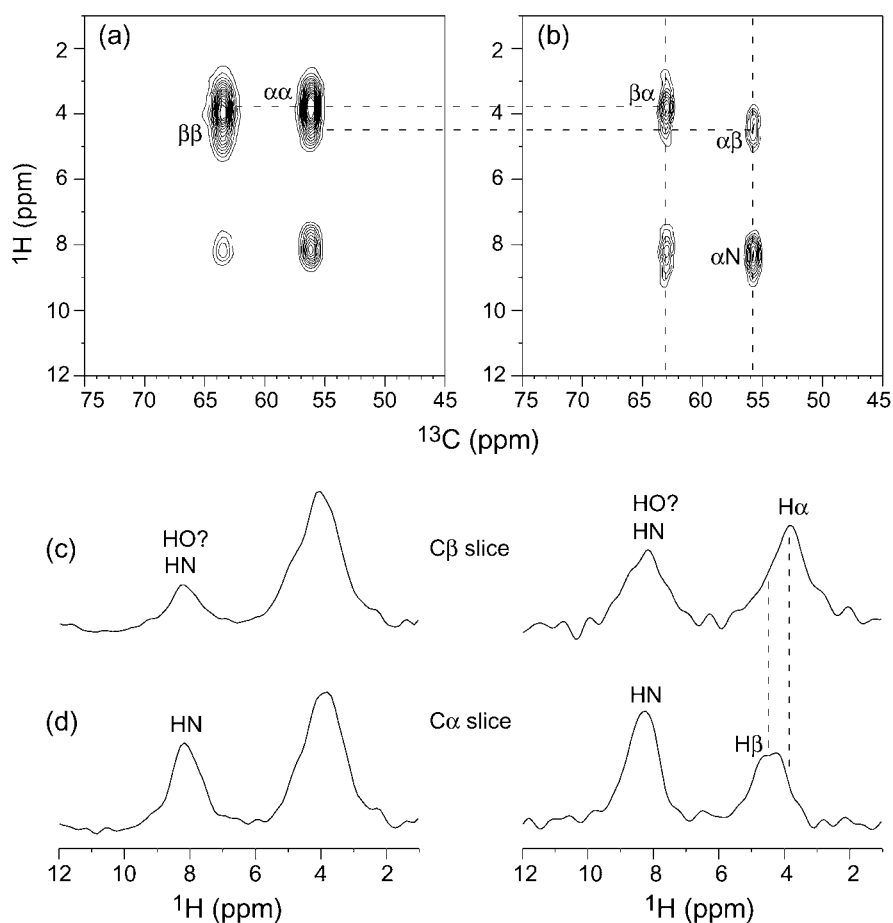


Figure 2.  $^1\text{H}$ - $^{13}\text{C}$  2D correlation spectra of Ser. (a) HETCOR spectrum, acquired with a LG-CP contact time of 1 ms, 64 scans per  $t_1$  slice, a  $^1\text{H}$  dwell time of 132  $\mu\text{s}$ , 128  $t_1$  slices, and a maximum  $^1\text{H}$  evolution time of 8.4 ms. (b) MELODI-HETCOR spectrum, acquired with a dipolar delay of 30  $\mu\text{s}$ , a LG-CP contact time of 1 ms, 80 scans per  $t_1$  slice, a  $^1\text{H}$  dwell time of 132  $\mu\text{s}$ , 56  $t_1$  slices, and a maximum  $^1\text{H}$  evolution time of 7.4 ms. The spinning speed for both experiments was 7576 Hz. The notation for assignment uses the first Greek letter for the carbon identity and the second Greek letter for the proton identity. (c)  $\text{C}\beta$  cross section from the HETCOR (left) and the MELODI-HETCOR (right) spectra. (d)  $\text{C}\alpha$  cross section from the HETCOR (left) and the MELODI-HETCOR (right) spectra.

unresolved in the HETCOR spectrum, but are clearly distinguished in the MELODI-HETCOR spectrum acquired with a 30  $\mu$ s filter. The H $\beta$  protons resonate at about 2.8 ppm, while the H $\alpha$  signal is centered at about 4.1 ppm.

In the aromatic region, three  $^{13}\text{C}$  signals corresponding to the quaternary C $\gamma$ , C $\delta$ 2, and C $\epsilon$ 1 are detected. The  $^{13}\text{C}$  assignment can be made only after comparing the HETCOR and the MELODI-HETCOR spectra. The most significant difference is the nearly complete suppression of the intensities in the 132 ppm and 111 ppm cross sections in the MELODI spectrum. This can only occur for C $\epsilon$ 1 and C $\delta$ 2, since they are relatively far from the proton-rich  $\beta$  and  $\alpha$  segments and reside in the proton-poor imidazole ring. The C $\epsilon$ 1 can be assigned to the downfield peak due to its association with the  $\epsilon$ 2 and  $\delta$ 1 nitrogens. The  $\delta$ 2 and  $\epsilon$ 1 carbons show only medium-range correlation peaks such as C $\delta$ 2-H $\beta$  in the MELODI-HETCOR spectrum. In comparison, the quaternary C $\gamma$  (135 ppm) receives all its magnetization from indirectly bonded protons and thus exhibits nearly identical intensity distributions between the HETCOR and the MELODI-HETCOR spectra. It is correlated with almost all protons in the molecule, including H $\beta$ , H $\alpha$ , H $\delta$ 2, and H $\delta$ 1. The upper limit of the C-H distances observable from these spectra can be estimated from the relatively weak correlation between C $\epsilon$ 1 and H $\beta$ . The crystal structure of histidine hydrochloride monohydrate, a related compound, shows C $\epsilon$ 1-H $\beta$  distances of 7.02 Å and 5.77 Å.

In the carbonyl slice, correlations with the aliphatic and amino protons are observed as expected. The resonance at 8–9 ppm may include not only the backbone amino protons but also the ring H $\delta$ 1 protons, since an intermolecular hydrogen bond between the carbonyl oxygen and H $\delta$ 1 is indicated by the crystal structure of histidine hydrochloride monohydrate. Figure 3e summarizes the medium- and long-range C-H correlations observed in His.

The  $^1\text{H}$  and  $^{13}\text{C}$  chemical shifts of the imidazole ring are very sensitive to the charge state. The presence of hydrochloride change the  $^1\text{H}$  and  $^{13}\text{C}$  chemical shifts significantly. The aromatic region of the unfiltered and filtered HETCOR spectra of histidine hydrochloride monohydrate (Figure 3c,d) indicate that protonation shifts the C $\delta$ 2 and C $\epsilon$ 1 resonances downfield by 8 ppm and 4 ppm, respectively, while the C $\gamma$  resonance is shifted upfield by 7 ppm, from 135 ppm in the neutral molecule to 128 ppm in the cationic state. Similarly, the  $^1\text{H}$  chemical shifts of H $\epsilon$ 1 and H $\delta$ 2

are displaced downfield by 2–3 ppm by the hydrochloride. Thus, the MELODI filter allows the measurement of both  $^1\text{H}$  and  $^{13}\text{C}$  chemical shift changes between different chemical modifications of His in the solid state.

### *Ubiquitin*

To demonstrate the improved resonance assignment of proteins achievable by the MELODI-HETCOR technique, we used [2- $^{13}\text{C}$ ]-glycerol S&E  $^{13}\text{C}$  labeled ubiquitin as a model system. The partial  $^{13}\text{C}$ -labeling approach provides a suitable test case, since it retains the signals of aliphatic protons that are bonded to unlabeled carbons in the MELODI-HETCOR spectra. A uniformly  $^{13}\text{C}$ -labeled protein, on the other hand, would dephase all aliphatic protons and retain only H $^{\text{N}}$  and OH signals.

### *Backbone region*

Figure 4 displays the  $^{13}\text{C}$ - $^1\text{H}$  HETCOR and MELODI-HETCOR spectra of S&E  $^{13}\text{C}$ -labeled ubiquitin (Hong, 1999). The HETCOR spectrum (Figure 4a) shows broad  $^1\text{H}$  resonances due to the overlap of many signals. The application of the  $^{13}\text{C}$ - $^1\text{H}$  MELODI filter significantly improved the  $^1\text{H}$  spectral resolution (Figure 4b). Most dramatic was the suppression of the C $\alpha$ -H $\alpha$  intensities. For example, the strong C $\alpha$ -H $\alpha$  intensities centered at ( $^{13}\text{C}$ ,  $^1\text{H}$ ) = (55.3 ppm, 4.5 ppm) were nearly completely suppressed in the MELODI-HETCOR spectrum, as were the Gly C $\alpha$ -H $\alpha$  intensities in the 45.4 ppm cross section. In comparison, the C $\alpha$ -H $\beta$  intensities at (55.3 ppm, 1.6 ppm) were retained in the MELODI-HETCOR spectrum. Based on previous  $^{15}\text{N}$ - $^{13}\text{C}$  correlation experiments (Hong, 1999), we assigned the  $^{13}\text{C}$  resonance at 51 ppm to Pro C $\delta$ . This cross section shows a broad intensity distribution in the HETCOR spectrum but a narrow peak centered at 2.2 ppm in the MELODI-HETCOR spectrum, which can be assigned to the two-bond Pro C $\delta$ -H $\gamma$  correlation. The assignment is confirmed by the lack of intensities between 8–9 ppm in the same cross section, since Pro residues do not possess an H $^{\text{N}}$ .

In the MELODI-HETCOR spectrum, no strong intensities were detected at the anticipated Ser C $\alpha$ -H $\beta$  position. This may partially result from the cancellation between the Ser C $\alpha$ -H $\alpha$  peak and the C $\alpha$ -H $\beta$  peak. Since the intensities of the one-bond correlation peaks depend sensitively on the MELODI filter time near the zero crossing, the dephased Ser C $\alpha$ -H $\alpha$  peak may have a slightly negative intensity, which would cancel the

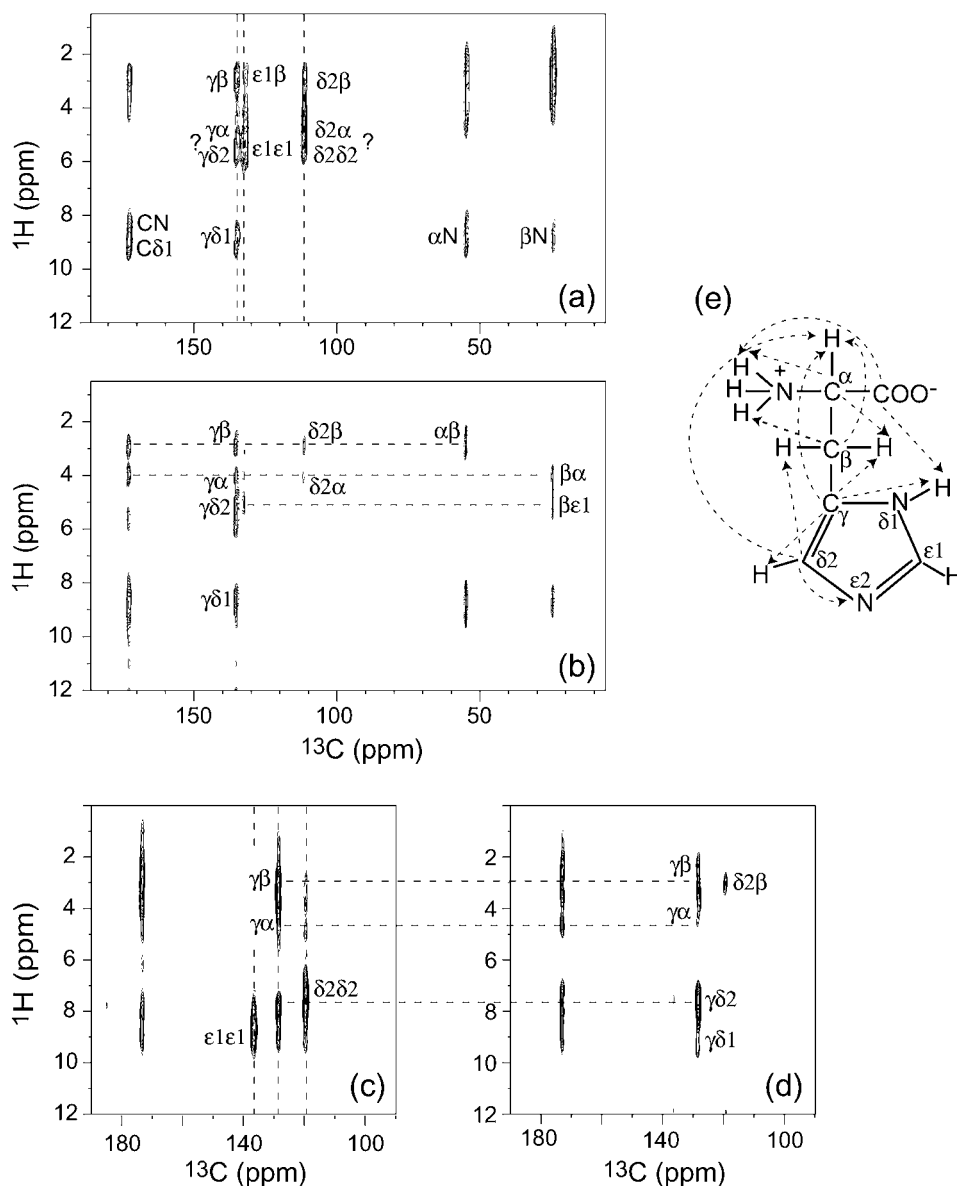
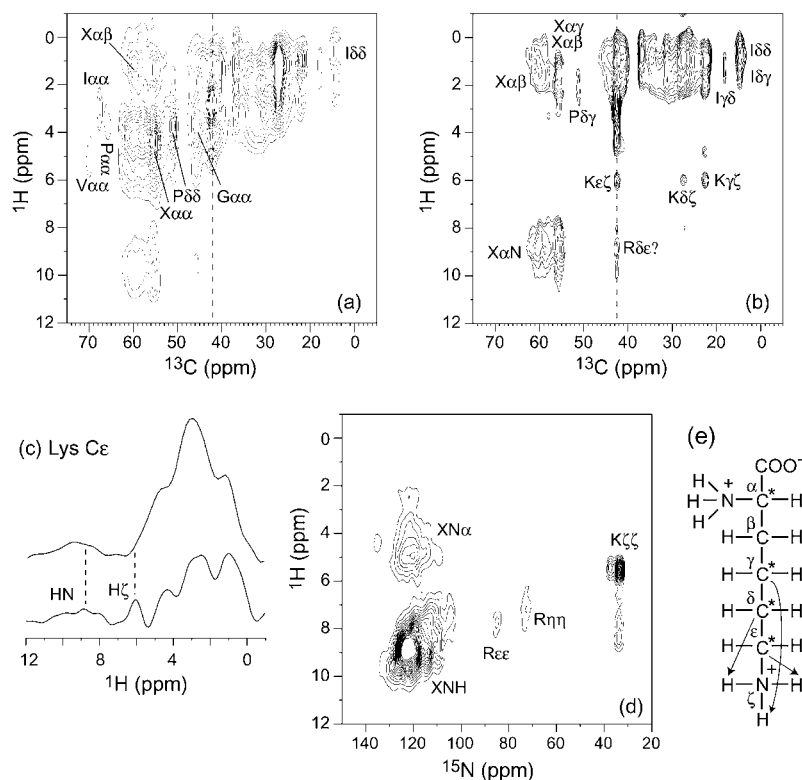


Figure 3. (a) HETCOR spectrum of His, acquired with a LG-CP contact time of 2.5 ms, 48 scans per  $t_1$  slice, a  $^1\text{H}$  dwell time of 132  $\mu\text{s}$ , 90  $t_1$  slices, and a maximum  $^1\text{H}$  evolution time of 5.94 ms. (b) MELODI-HETCOR spectrum of His, acquired with a dipolar delay of 30  $\mu\text{s}$ , a LG-CP contact time of 2.5 ms, 80 scans per  $t_1$  slice, a  $^1\text{H}$  dwell time of 132  $\mu\text{s}$ , 45  $t_1$  slices, and a maximum  $^1\text{H}$  evolution time of 5.94 ms. The spinning speed was 7576 Hz for both experiments. (c) HETCOR spectrum of histidine hydrochloride monohydrate, acquired with a  $^1\text{H}$  dwell time of 66  $\mu\text{s}$ , a maximum  $^1\text{H}$  evolution time of 4.7 ms, and a spinning speed of 5682 Hz. (d) MELODI-HETCOR spectrum of histidine hydrochloride monohydrate, acquired with a dipolar delay of 25  $\mu\text{s}$ , a  $^1\text{H}$  dwell time of 66  $\mu\text{s}$ , 64  $t_1$  slices, a maximum  $^1\text{H}$  evolution time of 4.2 ms, and a spinning speed of 6061 Hz. (e) Nomenclature for His and the detected medium- and long-range C-H correlations from these spectra.



**Figure 4.**  $^1\text{H}$ - $^{13}\text{C}$  2D correlation spectra of ubiquitin. (a) HETCOR spectrum, acquired with a LG-CP contact time of 1 ms, 80 scans per  $t_1$  slice, a  $^1\text{H}$  dwell time of 88  $\mu\text{s}$ , 88  $t_1$  slices, a maximum  $^1\text{H}$  evolution time of 3.8 ms, and a spinning speed of 9921 Hz. (b) MELODI-HETCOR spectrum, acquired with a dipolar delay of 15  $\mu\text{s}$ , a LG-CP contact time of 1 ms, 72 scans per  $t_1$  slice, a  $^1\text{H}$  dwell time of 88  $\mu\text{s}$ , 56  $t_1$  slices, a maximum  $^1\text{H}$  evolution time of 4.8 ms, and a spinning speed of 7576 Hz. (c) The Lys C $\epsilon$  (42.4 ppm) cross section from the HETCOR (top) and the MELODI-HETCOR (bottom) spectra. (d)  $^1\text{H}$ - $^{15}\text{N}$  HETCOR spectrum, acquired with a LG-CP contact time of 1 ms, 64 scans per  $t_1$  slice, a  $^1\text{H}$  dwell time of 132  $\mu\text{s}$ , 72  $t_1$  slices, a maximum  $^1\text{H}$  evolution time of 4.7 ms, and a spinning speed of 7576 Hz. (e) Nomenclatures for Lys and the observed medium- and long-range correlations from the  $^{13}\text{C}$ - $^1\text{H}$  and  $^{15}\text{N}$ - $^1\text{H}$  HETCOR spectra. Asterisks indicate the  $^{13}\text{C}$  labeled sites (Hong, 1999).

C $\alpha$ -H $\beta$  peak nearby. Such a negative C $\alpha$ -H $\alpha$  peak is observed in the spectrum of glutamine in Figure 6 (see below). In addition, the Ser C $\alpha$ -H $\beta$  peak is weakened by the partial labeling of C $\beta$ , which had been observed previously for this protein in a double-quantum  $^{13}\text{C}$  correlation spectrum (Hong, 1999). In comparison, the Ser C $\beta$ -H $\alpha$  correlation is not observed because of the 100% labeling of C $\alpha$  by  $[2\text{-}^{13}\text{C}]$  glycerol.

#### Side chain region

In the side chain carbon region of the ubiquitin MELODI-HETCOR spectrum, the  $^{13}\text{C}$ - $^1\text{H}$  correlation peaks of amino acids containing nitrogen atoms were accentuated. Most distinctly, a number of correlation peaks at a chemical shift of 6.0 ppm were observed. We assigned these peaks to the Lys NH $_3$  protons, since their  $^{13}\text{C}$  chemical shifts of 42.4 ppm, 27.4 ppm, and 22.4 ppm match the Lys C $\epsilon$ , C $\delta$ , and C $\gamma$ , respectively.

The Lys carbons are labeled by  $[2\text{-}^{13}\text{C}]$  glycerol at C $\alpha$ , C $\gamma$ , C $\delta$ , and C $\epsilon$  (Figure 4e). The assignment is consistent with the absence of a peak at 34 ppm, which is the average Lys C $\beta$  chemical shifts in ubiquitin (Wang et al., 1995). These non-bonded  $^{13}\text{C}$ - $^1\text{H}$  correlations of Lys are only weakly present in the conventional HETCOR spectrum, but are hardly resolved from the wings of the broad one-bond correlation peaks. The Lys C $\epsilon$  cross section (42.4 ppm) is shown in Figure 4c. The H $\zeta$  peak is nearly impossible to identify in the HETCOR spectrum, but becomes distinct and resolved in the MELODI-HETCOR cross section. In the Lys C $\delta$  and C $\gamma$  slices, the loss of intensities between 2.5 ppm and 4 ppm in the MELODI spectrum suggests that the H $\gamma$  and H $\delta$  chemical shifts are within this region.

To confirm the assignment of the Lys side chain protons, we carried out a  $^{15}\text{N}$ - $^1\text{H}$  HETCOR experiment (Figure 4d). By virtue of their distinctly up-

field  $^{15}\text{N}$  chemical shifts, the Lys  $\text{NH}_3$  group was unambiguously identified as the resonance at ( $^{15}\text{N}$ ,  $^1\text{H}$ ) = (33 ppm, 5.5 ppm). Interestingly, a second  $^1\text{H}$  signal at 8.3 ppm is also visible in the same  $^{15}\text{N}$  slice. This weaker signal may arise from inter-residue contacts made by the Lys  $\text{N}\zeta$  to the backbone amide protons of other residues. The small  $^1\text{H}$  chemical shift difference between the C-H and N-H HETCOR spectra probably results from the uncertainty in the FSLG scaling factor. The theoretical FSLG scaling factor of 0.577 was used in processing the 2D spectra, but the experimental scaling factor may deviate by a few percent.

It should be emphasized that the sensitivity enhancement of the long-range correlation peaks in the Lys side chain is relative to the one-bond correlation peaks. It results from the filtration of the  $^1\text{H}$  magnetization involved in the strong one-bond C-H dipolar couplings. The MELODI filter does not change the fact that both weak and strong C-H dipolar couplings are present in the Hamiltonian of the  $^1\text{H}$  spins of interest, and the weak dipolar couplings are truncated by the strong one. However, by removing the  $^1\text{H}$  magnetization involved in the strong coupling, the 2D spectra selectively detect the long-range correlation peaks of interest.

Similar to the Lys  $\text{NH}_3$  signals, the Arg guanidinium NH resonances can also be assigned in the  $^{15}\text{N}$ - $^1\text{H}$  HETCOR spectrum (Figure 4d). The  $\text{H}\eta$  and  $\text{H}\epsilon$  resonances appear at 7.2 ppm and 7.8 ppm, respectively. The corresponding signal in the  $^{13}\text{C}$ - $^1\text{H}$  MELODI-HETCOR spectrum is expected to appear at the Arg  $\text{C}\delta$  chemical shift, which, unfortunately, overlaps with the Lys  $\text{C}\epsilon$  peak. Thus, a conclusive assignment for Arg side chain carbons cannot be made. But we expect the intensities at (42 ppm, 8.5 ppm) to have partial contributions from the Arg  $\text{H}\epsilon$  and  $\text{H}\eta$ .

The most upfield  $^{13}\text{C}$  signals (14.5 ppm and 18.0 ppm) in both C-H HETCOR spectra of ubiquitin belong to Ile methyl  $\text{C}\delta$ . Due to the fast 3-site jumps of methyl groups, the C-H dipolar couplings are partially averaged, thus the methyl proton intensities were not completely suppressed by the MELODI filter. The carbonyl region (not shown) also shows little intensity differences between the two spectra, as expected since the carbonyl carbons have no directly bonded protons and all their cross peaks must be retained in the MELODI-HETCOR spectra.

Together, the  $^{15}\text{N}$ - $^1\text{H}$  and  $^{13}\text{C}$ - $^1\text{H}$  HETCOR and MELODI-HETCOR spectra of ubiquitin provide clear assignment of the residues with side chain nitrogen

atoms. This information was previously not available from other backbone based  $^{13}\text{C}$ - $^{15}\text{N}$  correlation experiments (Hong, 1999; Straus et al., 1998) or  $^{13}\text{C}$ - $^{13}\text{C}$  correlation experiments (McDermott et al., 2000).

#### *Colicin Ia channel domain*

The TEASE- $^{13}\text{C}$  labeled colicin Ia channel domain (22 kDa) provides an excellent example where more selective labeling further simplifies the analysis of the  $^1\text{H}$ - $^{13}\text{C}$  correlation spectra. The TEASE  $^{13}\text{C}$ -labeled sites in the protein include H ( $\delta 2$ ), S ( $\alpha$ ), G ( $\alpha$ ), C ( $\alpha$ ), W ( $\alpha$ ,  $\delta 2$ ,  $\zeta 3$ ), F ( $\alpha$ ,  $\gamma$ ,  $\epsilon 1$ ), Y ( $\alpha$ ,  $\gamma$ ,  $\epsilon 1$ ), A ( $\alpha$ ), V ( $\alpha$ ,  $\beta$ ), and L ( $\beta$ ,  $\gamma$ , CO) (Hong and Jakes, 1999). Out of 189 residues in colicin, only 110 residues were labeled (Hong and Jakes, 1999), making the NMR-observable part of the protein only 40% larger than ubiquitin rather than 2.5 times larger. Many of these  $^{13}\text{C}$  signals are observed in the normal HETCOR spectra of the soluble colicin (Figure 5a). For example, the backbone  $\text{C}\alpha$ - $\text{H}\alpha$  peaks of Val, Ala and Gly are readily assigned, several aromatic signals from Phe, His, and Tyr can be identified, and side chain correlation peaks in Leu and Val are also seen. However, the less distinct  $\text{C}\alpha$  shifts of Ser and Phe residues cannot be assigned in the HETCOR spectrum. Overall, the amino acid-type resolution of the colicin spectrum is significantly higher than that of ubiquitin. This results partly from the reduced number of amino acid types labeled in the protein, and partly from the high helical content of the protein (Wiener et al., 1997), which reduces the chemical shift dispersion.

Upon the application of the C-H MELODI filter, the backbone region of the spectrum (Figure 5b) exhibits the remaining  $\text{C}\alpha$ - $\text{H}\beta$  and  $\text{C}\alpha$ - $\text{H}\gamma$  peaks of Val residues, while the  $\text{C}\alpha$ - $\text{H}\alpha$  peaks, for example of Ala (53.2 ppm) and Val (64.0 ppm) residues, were strongly suppressed (Figure 5c). Comparing this spectrum with the Ser MELODI-HETCOR spectrum, we suggest the resonance at (59.8 ppm, 3.6 ppm) to be Ser  $\text{C}\alpha$ - $\text{H}\beta$ . Its equivalent position in the HETCOR spectrum is part of a broad  $^1\text{H}$  intensity distribution from 2.5 ppm to 5 ppm, which is impossible to assign. We can also tentatively assign the Phe  $\text{H}\beta$  chemical shift to be 3.0 ppm, since correlation peaks at 3.0 ppm were detected in the Phe  $\text{C}\epsilon 2$  (128.3 ppm) and  $\text{C}\gamma$  (137.7 ppm) cross sections. However, we cannot identify the Phe  $\text{C}\alpha$ - $\text{H}\beta$  peaks, possibly due to a low  $\text{C}\alpha$  labeling level and residual resonance overlap.

While the side chain region of the colicin MELODI-HETCOR spectrum shows better  $^1\text{H}$  reso-



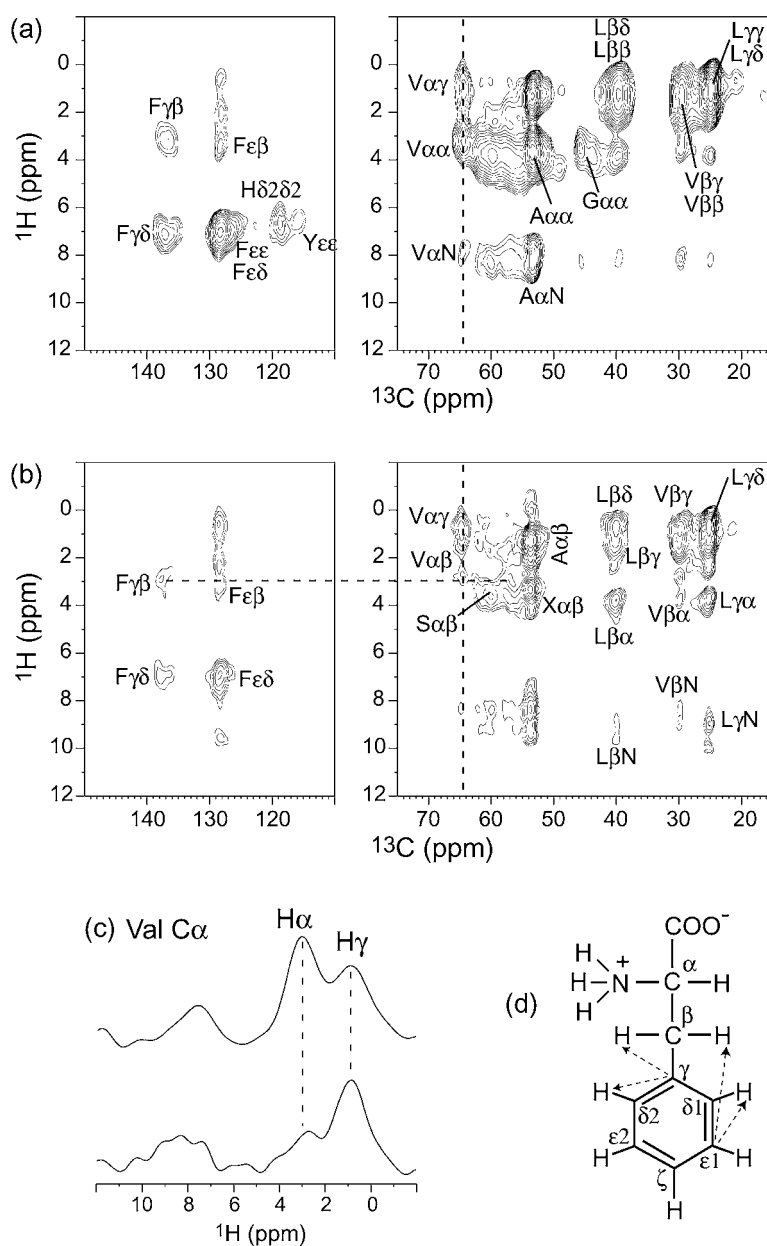


**Figure 5.**  $^1\text{H}$ - $^{13}\text{C}$  2D correlation spectra of TEASE  $^{13}\text{C}$ -labeled colicin Ia channel domain in the soluble form. (a) HETCOR spectrum, acquired with a LG-CP contact time of 1 ms, 88 scans per  $t_1$  slice, a  $^1\text{H}$  dwell time of 88  $\mu\text{s}$ , 72  $t_1$  slices, and a maximum  $^1\text{H}$  evolution time of 3.1 ms. (b) MELODI-HETCOR spectrum, acquired with a dipolar delay of 15  $\mu\text{s}$ , a LG-CP contact time of 1 ms, 160 scans per  $t_1$  slice, a  $^1\text{H}$  dwell time of 88  $\mu\text{s}$ , 54  $t_1$  slices, and a maximum  $^1\text{H}$  evolution time of 4.7 ms. The spinning speed was 7576 Hz. (c) Val C $\alpha$  (64 ppm) cross sections from the HETCOR (top) and the MELODI-HETCOR (bottom) spectra. (d) Nomenclature for Phe and the observed medium- and long-range correlations. The  $^{13}\text{C}$ -labeled sites are: H ( $\delta 2$ ), S ( $\alpha$ ), G ( $\alpha$ ), C ( $\alpha$ ), W ( $\alpha$ ,  $\delta 2$ ,  $\zeta 3$ ), F ( $\alpha$ ,  $\gamma$ ,  $\epsilon 1$ ), Y ( $\alpha$ ,  $\gamma$ ,  $\epsilon 1$ ), A ( $\alpha$ ), V ( $\alpha$ ,  $\beta$ ), and L ( $\beta$ ,  $\gamma$ , CO) (Hong and Jakes, 1999).

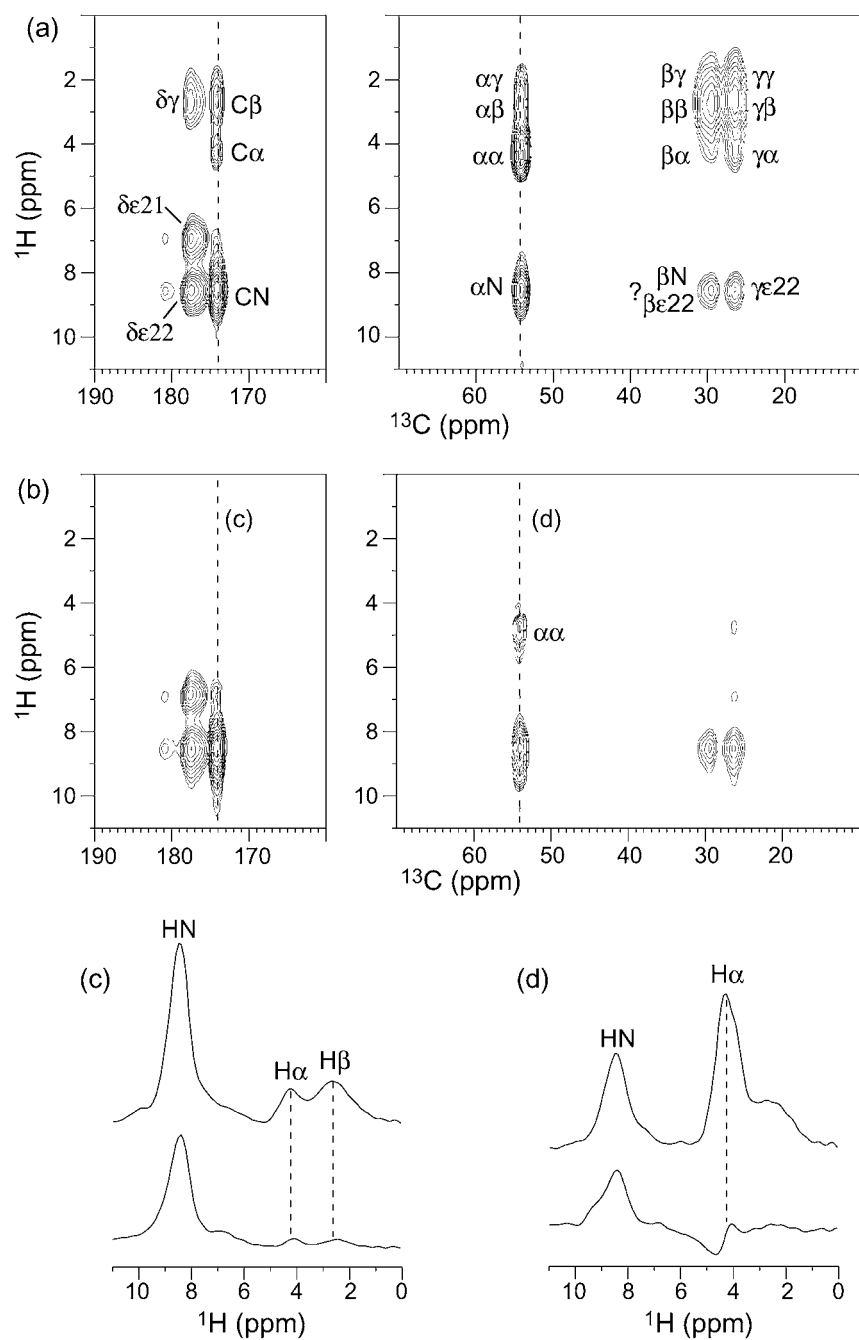


Figure 6.  $^1\text{H}$ - $^{13}\text{C}$  2D correlation spectra of  $^1\text{H}$ - $^{13}\text{C}$ ,  $^{15}\text{N}$ -labeled Gln. (a) HETCOR spectrum, acquired with a LG-CP contact time of 500  $\mu\text{s}$ , 8 scans per  $t_1$  slice, a  $^1\text{H}$  dwell time of 88  $\mu\text{s}$ , 192  $t_1$  slices, and a maximum  $^1\text{H}$  evolution of 8.4 ms.  $\epsilon 22$  and  $\epsilon 21$  refers to the side chain amide proton *cis* and *trans* to the carbonyl oxygen, respectively. (b) MELODI-HETCOR spectrum, acquired with a dipolar filter delay of 17  $\mu\text{s}$ , a LG-CP contact time of 500  $\mu\text{s}$ , 16 scans per  $t_1$  slice, a  $^1\text{H}$  dwell time of 88  $\mu\text{s}$ , 96  $t_1$  slices, and a maximum  $^1\text{H}$  evolution time of 8.4 ms. (c) Carbonyl carbon (174 ppm) cross section from the HETCOR (top) and the MELODI-HETCOR (bottom) spectra. (d)  $\text{C}\alpha$  (54 ppm) cross section from the HETCOR (top) and the MELODI-HETCOR (bottom) spectra. The spinning speed for both experiments was 7576 Hz.

lution than the HETCOR spectrum, the suppression of the one-bond correlation peaks is incomplete due to the presence of motions that weaken the C-H dipolar couplings (Huster et al., 2001). This is true for the Leu C $\beta$  (39.7 ppm) and Val C $\beta$  (29.6 ppm). The carbons with neighboring methyl protons, including Val C $\beta$  and Leu C $\gamma$ , are the least filtered, since the fast 3-site jumps reduce the directly bonded C-H dipolar couplings that drive the MELODI filtration.

In the aromatic region, the quaternary C $\gamma$  of Phe (137.7 ppm) has only medium- and long-range cross peaks. These are preserved in both the unfiltered and filtered spectra. The Phe C $\epsilon$  (128.3 ppm) cross section is similar between the two spectra, because the H $\epsilon$  and H $\delta$  chemical shifts are very close. The  $^{13}\text{C}$  cross section at 118.7 ppm can be attributed to His C $\delta 2$ . It shows a C $\delta 2$ -H $\delta 2$  cross peak in the HETCOR spectrum that was suppressed in the MELODI-HETCOR spectrum. This is fully consistent with the spectra of the amino acid His (Figure 3). Finally, a weak Tyr C $\epsilon$ -H $\epsilon$  signal was assigned in the HETCOR spectrum but suppressed in the MELODI-HETCOR spectrum.

The dipolar MELODI-HETCOR technique is exactly complementary to the J-coupling based polarization transfer techniques (Lesage et al., 1998). While J-coupled correlation spectra are highly selective of directly bonded nuclei and thus have good site resolution, their use for protein resonance assignment is limited by the lack of distinction among the backbone atoms of different amino acids. The utilization of side chain chemical shifts by J-spectroscopy requires long polarization transfer times, which reduce the experimental sensitivity (Lesage et al., 2000). The MELODI-HETCOR experiment, on the other hand, efficiently selects the peaks correlating indirectly bonded nuclei, thus achieves amino acid type assignment and resolution enhancement simultaneously.

#### *Uniformly $^{13}\text{C}$ , $^{15}\text{N}$ labeled glutamine*

While the MELODI-HETCOR technique is most suitable for partially labeled and natural abundance systems, it can also be applied to uniformly  $^{13}\text{C}$ -labeled proteins to selectively detect protons not bonded to carbons, since the  $^{13}\text{C}$ - $^1\text{H}$  dipolar filter will leave the NH, OH, and SH proton magnetization intact. Half of the twenty amino acids, including Gln, Asn, Lys, Arg, Thr, Ser, Tyr, His, Trp, and Cys, contain such protons in their side chains. These unique protons can be

exploited by the MELODI technique to identify these amino acids.

Figure 6 shows the  $^{13}\text{C}$ - $^1\text{H}$  correlation spectra of uniformly  $^{13}\text{C}$  and  $^{15}\text{N}$  labeled Gln. The normal HETCOR spectrum was acquired with a LG-CP contact time of 500  $\mu\text{s}$ , which was sufficiently long to detect both two- and three-bond correlation peaks such as C $\alpha$ -H $^{\text{N}}$  and C $\beta$ -H $^{\text{N}}$ , and one-bond correlation peaks. In the carbonyl region, all cross peaks originated from indirectly bonded spin pairs. The side chain C $\delta$  exhibits two distinct H $\epsilon$  signals, since the amide protons *cis* ( $\epsilon 22$ ) and *trans* ( $\epsilon 21$ ) to the carbonyl oxygen experience different electronic environments.

The application of the  $^{13}\text{C}$ - $^1\text{H}$  MELODI filter suppressed the intensities of most aliphatic protons in Gln (Figure 6b). Only a weakly negative C $\alpha$ -H $\alpha$  peak was detected below 6 ppm in the  $^1\text{H}$  dimension. This indicates that the one-bond C-H dipolar oscillation had crossed zero and become negative at the filter time used, which was 17  $\mu\text{s}$  out of a rotor period of 132  $\mu\text{s}$ . All other aliphatic  $^1\text{H}$  signals were completely suppressed. Above 6 ppm, all NH proton signals remain. Figures 6c and d compare the backbone carbonyl and C $\alpha$  cross sections of the HETCOR and MELODI-HETCOR spectra. This method of suppressing CH protons and retaining NH protons may be useful for selective excitation of the H $^{\text{N}}$  magnetization in proteins.

## Conclusions and outlook

We have shown that the MELODI filter considerably simplifies the  $^{13}\text{C}$ - $^1\text{H}$  correlation spectra by removing the one-bond C-H correlation peaks and thus enhancing the  $^1\text{H}$  spectral resolution. It can be considered a heteronuclear analog of the homonuclear double-quantum filtered COSY-type of experiments (Geen et al., 1997; Piantini et al., 1982; Rance et al., 1983; Rienstra et al., 1998), which filters out the diagonal peaks to facilitate the assignment of cross peaks close to the diagonal.

In amino acids, the MELODI filter allowed us to distinguish  $^1\text{H}$  signals with chemical shift differences of only 0.6 ppm, and correctly identified the reversal of H $\alpha$  and H $\beta$  chemical shifts in Ser. Application to His yielded complete  $^{13}\text{C}$  assignment and most of the  $^1\text{H}$  assignment. It further allowed the determination of the  $^1\text{H}$  and  $^{13}\text{C}$  chemical shift differences between the neutral and cationic imidazole ring. Such MELODI-HETCOR spectra of individual amino acids can serve

as useful fingerprints to facilitate the amino acid type assignment of protein spectra.

For extensively  $^{13}\text{C}$ -labeled ubiquitin, the MELODI-HETCOR spectra provided the assignment of Lys residues, since their  $\text{H}\zeta$  amino protons were not suppressed by the C-H dipolar filter. The Lys side chain assignment was confirmed by an  $^{15}\text{N}$ - $^1\text{H}$  HETCOR experiment, which also yielded Arg guanidinium  $^1\text{H}$  chemical shifts. The  $^{13}\text{C}$ - $^1\text{H}$  MELODI-HETCOR spectrum of colicin Ia channel domain allowed the tentative assignment of Ser, which have indistinct  $\text{C}\alpha$  chemical shifts. Clearly, the inherent overlap in the 2D spectra of these realistically sized and extensively labeled proteins restricts the assignment to that of the amino-acid types. More complete assignment is well possible, if more specific labeling schemes, more careful sample preparation protocols, and three-dimensional correlation spectroscopy are employed.

The MELODI-HETCOR technique is expected to be most suitable for partially labeled proteins. One labeling strategy involves 100% labeling of certain carbons in each amino acid while keeping the others completely unlabeled. The TEASE protocol with site-specifically labeled glycerol as the precursor is an example of this approach. Alternatively, fractionally labeled proteins also offer interesting possibilities. There, the auto-correlation peaks will still be completely suppressed, but all cross correlation peaks such as  $\text{C}\alpha$ - $\text{H}\beta$  and  $\text{C}\beta$ - $\text{H}\alpha$  should be present. The spectra will be analogous to those of the natural abundance Ser and His, but with higher sensitivities.

On the other hand, even with uniform  $^{13}\text{C}$  labeling, the NH, OH, SH signals and the mobile methyl proton signals still remain in the MELODI-HETCOR spectra. We demonstrated here the distinct MELODI fingerprint of U- $^{13}\text{C}$ ,  $^{15}\text{N}$ -labeled Gln. The spectra suggest that residues such as Lys, Arg, Trp, and Asn may be possible to assign in this way.

Finally, the sensitivity of both the HETCOR and MELODI-HETCOR experiments is high. For the unlabeled amino acids, acquisition times as short as 3 h were used, while for the labeled proteins with limited sample amounts, the acquisition times ranged from 3.5 h to 8 h. Thus, these are efficient experiments that can be readily incorporated into the repertoire of correlation techniques for resonance assignment of solid proteins.

## Acknowledgements

M.H. gratefully acknowledges the Arnold and Mabel Beckman Foundation for a Young Investigator Award and Petroleum Research Fund for financial support.

## References

- Caravatti, P., Braunschweiler, L. and Ernst, R.R. (1983) *Chem. Phys. Lett.*, **100**, 305–310.
- Geen, H., Gottwald, J., Graf, R., Schnell, I., Spiess, H.W. and Titman, J.J. (1997) *J. Magn. Reson.*, **125**, 224–227.
- Hong, M. (1999a) *J. Magn. Reson.*, **139**, 389–401.
- Hong, M. (1999b) *J. Biomol. NMR*, **15**, 1–14.
- Hong, M. and Griffin, R.G. (1998) *J. Am. Chem. Soc.*, **120**, 7113–7114.
- Hong, M. and Jakes, K. (1999) *J. Biomol. NMR*, **14**, 71–74.
- Huster, D., Xiao, L.S. and Hong, M. (2001) *Biochemistry*, accepted.
- Ishii, Y. and Tycko, R. (2000) *J. Am. Chem. Soc.*, **122**, 1443–1455.
- Lee, C.W.B. and Griffin, R.G. (1989) *Biophys. J.*, **55**, 355–358.
- Lee, M. and Goldberg, W.I. (1965) *Phys. Rev.*, **140**, A1261–A1271.
- Lesage, A., Charmont, P., Steuernagel, S. and Emsley, L. (2000) *J. Am. Chem. Soc.*, **122**, 9739–9744.
- Lesage, A., Sakellariou, D., Steuernagel, S. and Emsley, L. (1998) *J. Am. Chem. Soc.*, **120**, 13194–13201.
- Marassi, F.M. and Opella, S.J. (2000) *J. Magn. Reson.*, **144**, 150–155.
- McDermott, A.E., Polenova, T., Bockmann, A., Zilm, K.W., Paulson, E.K., Martin, R.W. and Montelione, G.T. (2000) *J. Biomol. NMR*, **16**, 209–219.
- Pauli, J., van Rossum, B., Forster, H., de Groot, H.J.M. and Oschkinat, H. (2000) *J. Magn. Reson.*, **143**, 411–416.
- Piantini, U., Sorensen, O.W. and Ernst, R.R. (1982) *J. Am. Chem. Soc.*, **104**, 6800–6801.
- Rance, M., Sorensen, O.W., Bodenhausen, G., Wagner, G., Ernst, R.R. and Wüthrich, K. (1983) *Biochem. Biophys. Res. Commun.*, **117**, 479–485.
- Rienstra, C.M., Hatcher, M.E., Mueller, L.J., Sun, B.Q., Fesik, S.W. and Griffin, R.G. (1998) *J. Am. Chem. Soc.*, **120**, 10602–10612.
- Rienstra, C.M., Hohwy, M., Hong, M. and Griffin, R.G. (2000) *J. Am. Chem. Soc.*, **122**, 10979–10990.
- Straus, S.K., Bremi, T. and Ernst, R.R. (1998) *J. Biomol. NMR*, **12**, 39–50.
- Tan, W.M., Gu, Z., Zeri, A.C. and Opella, S.J. (1999) *J. Biomol. NMR*, **13**, 337–342.
- van Rossum, B.J., de Groot, C.P., Ladizhansky, V., Vega, S. and de Groot, H.J.M. (2000) *J. Am. Chem. Soc.*, **122**, 3465–3472.
- van Rossum, B.J., Forster, H. and de Groot, H.J.M. (1997) *J. Magn. Reson.*, **124**, 516–519.
- Vinogradov, E., Madhu, P.K. and Vega, S. (1999) *Chem. Phys. Lett.*, **314**, 443–450.
- Wang, A.C. and Bax, A. (1996) *J. Am. Chem. Soc.*, **118**, 2483–2494.
- Wang, A.C., Grzesiek, S., Tschudin, R., Lodi, P.J. and Bax, A. (1995) *J. Biomol. NMR*, **5**, 376–382.
- Wang, J., Denny, J., Tian, C., Kim, S., Mo, Y., Kovacs, F., Song, Z., Nishimura, K., Gan, Z., Fu, R., Quine, J.R. and Cross, T.A. (2000) *J. Magn. Reson.*, **144**, 162–167.
- Wiener, M., Freymann, D., Ghosh, P. and Stroud, R.M. (1997) *Nature*, **385**, 461–464.
- Wüthrich, K. (1986) *NMR of Proteins and Nucleic Acids*, John Wiley, New York, NY.
- Yao, X.L., Schmidt-Rohr, K. and Hong, M. (2001) *J. Magn. Reson.*, **149**, 139–143.